

## Journal Pre-proofs

Continuous lactate-driven dark fermentation of restaurant food waste: Process characterization and new insights on transient feast/famine perturbations

Lois Regueira-Marcos, Raúl Muñoz, Octavio García-Depraect

PII: S0960-8524(23)00811-8  
DOI: <https://doi.org/10.1016/j.biortech.2023.129385>  
Reference: BITE 129385

To appear in: *Bioresource Technology*

Received Date: 3 May 2023  
Revised Date: 19 June 2023  
Accepted Date: 20 June 2023



Please cite this article as: Regueira-Marcos, L., Muñoz, R., García-Depraect, O., Continuous lactate-driven dark fermentation of restaurant food waste: Process characterization and new insights on transient feast/famine perturbations, *Bioresource Technology* (2023), doi: <https://doi.org/10.1016/j.biortech.2023.129385>

This is a PDF file of an article that has undergone enhancements after acceptance, such as the addition of a cover page and metadata, and formatting for readability, but it is not yet the definitive version of record. This version will undergo additional copyediting, typesetting and review before it is published in its final form, but we are providing this version to give early visibility of the article. Please note that, during the production process, errors may be discovered which could affect the content, and all legal disclaimers that apply to the journal pertain.

© 2023 The Author(s). Published by Elsevier Ltd.

1       **Continuous lactate-driven dark fermentation of restaurant food waste: Process**  
2       **characterization and new insights on transient feast/famine perturbations**

3           Lois Regueira-Marcos <sup>a, b</sup>, Raúl Muñoz <sup>a, b</sup>, Octavio García-Depraect <sup>a, b\*</sup>

4  
5       <sup>a</sup> Institute of Sustainable Processes, University of Valladolid, Dr. Mergelina, s/n, 47011,  
6       Valladolid Spain

7       <sup>b</sup> Department of Chemical Engineering and Environmental Technology, School of  
8       Industrial Engineering, University of Valladolid, Dr. Mergelina, s/n, 47011, Valladolid  
9       Spain

10  
11       \***Corresponding author:** Dr. Octavio García Depraect; **E-mail address:**  
12       octavio.garcia@uva.es; **Full postal address:** Institute of Sustainable Processes,  
13       University of Valladolid, Dr. Mergelina, s/n, 47011, Valladolid Spain

14  
15       **Abstract**

16       The effect of hydraulic retention time (HRT) on the continuous lactate-driven dark  
17       fermentation (LD-DF) of food waste (FW) was investigated. The robustness of the  
18       bioprocess against feast/famine perturbations was also explored. The stepwise HRT  
19       decrease from 24 to 16 and 12 h in a continuously stirred tank fermenter fed with  
20       simulated restaurant FW impacted on hydrogen production rate (HPR). The optimal  
21       HRT of 16 h supported a HPR of 4.2 L H<sub>2</sub>/L-d. Feast/famine perturbations caused by  
22       12-h feeding interruptions led to a remarkable peak in HPR up to 19.2 L H<sub>2</sub>/L-d, albeit  
23       the process became stable at 4.3 L H<sub>2</sub>/L-d following perturbation. The occurrence of  
24       LD-DF throughout the operation was endorsed by metabolites analysis. Particularly,  
25       hydrogen production positively correlated with lactate consumption and butyrate  
26       production. Overall, the FW LD-DF process was highly sensitive but resilient against  
27       transient feast/famine perturbations, supporting high-rate HPRs under optimal HRTs.

28  
29       **Keywords:**

30       Acidogenic fermentation, Biogenic hydrogen, Hydraulic retention time, Organic waste,  
31       Process disturbances, Robustness.

32  
33       **1. Introduction**

34 Renewable hydrogen produced from biomass via biochemical conversion processes is  
35 gaining momentum in the European Union and beyond, since it fosters the  
36 decarbonisation of energy-intensive industrial processes and the transition towards a  
37 circular economy (European Commission, 2020). Hydrogen can not only be used as a  
38 clean energy carrier, but it can also be an industrial feedstock (European Commission,  
39 2020; Dawood et al., 2020). Dark fermentation (DF) stands out as the most promising  
40 biological method to produce renewable hydrogen, owing to its potentially higher  
41 hydrogen production yields (HY) and rates (HPR), and good flexibility in using a wide  
42 range of different organic wastewaters and wastes (Cheng et al., 2022). In this context,  
43 food waste (FW) has attracted an increasing attention as a biorefinery feedstock due to  
44 its year-round availability and physicochemical features, conferring it a high potential  
45 for producing added-value compounds and energy carriers including hydrogen via  
46 microbial fermentation processes (Zabaniotou & Kamaterou, 2019; Battista et al., 2020;  
47 Talan et al., 2021; Shanmugan et al., 2023)). To date, one third of the food produced  
48 worldwide ends up as FW, which in turn causes serious environmental, social and  
49 health issues (Scherhauser et al., 2018; Fattibene et al., 2020; Shanmugan et al., 2023).  
50 In the European Union, this figure accounted for 56.8 million tons in 2020,  
51 corresponding to about 127 kg of FW generated per inhabitant (Eurostat, 2022). The  
52 North America, Latin America and Caribbean, sub-Saharan Africa and Asia-Pacific  
53 regions generate yearly about 168, 127, 232 and 465 million tons of FW, respectively  
54 (García-Depraect et al., 2023b).

55 Although DF has long been proven as a feasible technology to produce hydrogen  
56 from FW (Yun et al., 2018; Habashy et al., 2021), its development and further scale up  
57 is still limited by several technical bottlenecks. Of them, the inhibition of hydrogen  
58 production caused either directly or indirectly by the overgrowth of lactic acid bacteria  
59 (LAB) in DF systems remains one of the most prevalent and deleterious issues (García-  
60 Depraect et al., 2021). Indeed, the proliferation of LAB has been considered the main  
61 cause of process collapse in the long-term operation of continuous DF processes. LAB  
62 often outcompete hydrogen-producing bacteria (HPB) due to their wider capacity to  
63 degrade complex substrates and because they can release antimicrobial compounds  
64 (Sikora et al., 2013; García-Depraect et al., 2021). Besides, LAB such as *Lactobacillus*  
65 and lactate-oxidizing-HPB such as *Clostridium butyricum*, share similar physical and  
66 chemical growth requirements, thus it is quite challenging to keep LAB away from the  
67 DF process by modulating process parameters such as the hydraulic retention time  
68 (HRT), organic loading rate (OLR), temperature, and pH (García-Depraect et al., 2021).  
69 Another aspect contributing to the common occurrence of LAB in dark fermenters is  
70 their ubiquitous nature, being part of the autochthonous microbiota of many organic  
71 feedstocks including FW. Indeed, the microbial community structure of FW is typically  
72 dominated by LAB during its storage (García-Depraect et al., 2023b).

73 Unfortunately, the effective elimination of LAB from the DF of FW still  
74 presents serious technical and economic issues, since pre-treatments intended to that  
75 purpose (heat shock for instance) are not only typically costly but have also been shown  
76 to be impractical and inefficient (Villanueva-Galindo et al., 2023). In this context,  
77 lactate-driven DF (LD-DF) is recently attracting scientific attention as a platform able to  
78 produce hydrogen from FW, while tackling the overgrowth of LAB (Regueira-Marcos  
79 et al., 2023). Although LD-DF is seen as a non-conventional hydrogen-producing

80 pathway, its prevalence in dark fermenters seems thermodynamically efficient, which is  
81 desirable in shaping stable microbial communities in the long run operation (Fuess et  
82 al., 2018). It has been argued that the long-lasting functional ecosystem in LD-DF is  
83 driven by syntrophic (cross-feeding) interactions between LAB and some HPB, in  
84 which the former microbial group ferment carbohydrates into lactate, while the latter  
85 transforms lactate into hydrogen (García-Depraect et al., 2021). This process would  
86 benefit both microbial groups, as lactate can be consumed by certain HPB avoiding  
87 deleterious LAB growth by product inhibition, while preventing competition between  
88 LAB and HPB for the fermentable carbohydrates (Park et al., 2021; Pérez-Rangel et al.,  
89 2021; Ohnishi et al., 2022). Despite the potential of this syntrophic microbial  
90 association to boost hydrogen production, the fate of lactate in the DF process is usually  
91 overlooked in most studies (Detman et al., 2019; García-Depraect et al., 2021; Ohnishi  
92 et al., 2022). In the case of LD-DF of FW, this has not been extensively investigated,  
93 thus many relevant insights remain unrevealed yet. To the best of the authors'  
94 knowledge, the process performance of the LD-DF of FW under continuous operation  
95 has not been systematically investigated yet. In continuous DF systems, HRT is likely  
96 the most critical process parameter determining the hydrogen production efficiency, in  
97 terms of HY and HPR (Sivagurunathan et al., 2016).

98 Hence, this work investigated for the first time the influence of the HRT on the  
99 continuous LD-DF of simulated restaurant FW. Additionally, the robustness and  
100 resilience of this novel LD-DF technology was assessed by characterizing process  
101 response to short-term feast/famine perturbations, which are foreseen to occur in full  
102 scale DF facilities and might compromise hydrogen production. The results and  
103 discussion of this study can be helpful in the development and deployment of  
104 enhancement strategies aimed at harnessing the presence of LAB in dark fermenters.

105

## 106 **2. Materials and Methods**

### 107 **2.1 Microbial inoculum and feedstock**

108 The inoculum source was digestate collected from a well-performing 100-L anaerobic  
109 digester fed with restaurant FW and operated under mesophilic conditions. A hydrogen-  
110 producing mixed culture was obtained by applying a heat shock pretreatment (90 °C for  
111 20 min) followed by three consecutive subcultures, following the procedure reported by  
112 Martínez-Mendoza et al. (2022). The resulting acidogenic culture was composed of  
113 *Lactobacillus*, *Klebsiella*, *Clostridium*, *Stenotrophomonas*, *Acinetobacter*, among others  
114 (Regueira-Marco et al., 2023). Then it was stored at 4 °C and used on-demand as  
115 inoculum for LD-DF (García-Depraect et al., 2022; Regueira-Marcos et al., 2023). Prior  
116 to use and with the aim of reactivating microorganisms, the bacterial inoculum was  
117 subjected to a 17-h fermentation step using a 2.1-L gas-tight anaerobic reactor filled  
118 with 0.1 L of inoculum and 0.9 L of a growth medium composed of (in g/L): 10.0  
119 lactose, 2.40 NH<sub>4</sub>Cl, 2.4 K<sub>2</sub>HPO<sub>4</sub>, 1.18 MgCl<sub>2</sub>, 0.60 KH<sub>2</sub>PO<sub>4</sub>, 0.11 CaCl<sub>2</sub>, and 0.024  
120 FeCl<sub>2</sub> (Martínez-Mendoza et al., 2022). The incubation conditions applied were 37 ± 1  
121 °C and ≈ 200 rpm.

122 The feedstock herein used was simulated FW prepared according to Neves et al.  
123 (2008), which mimics the composition of restaurant-derived FW. That formulation  
124 included 78% potatoes, 14% chicken, 4% pork lard, and 4% cabbage (on wet weight  
125 basis), as the source of carbohydrate, protein, lipid, and fiber, respectively. Potatoes and  
126 chicken breast were boiled in an autoclave at 120 °C for 30 min to simulate cooked FW.  
127 The FW was initially blended by using a commercial blender (Sammic, XM-32, Spain)  
128 and subsequently stored at -20 °C to prevent any change in its composition. The  
129 microbial community structure of the recipe-based FW used has been reported  
130 previously by García-Depraect et al. (2023b). The blended FW was physiochemically  
131 characterized as follows:  $51.0 \pm 0.5\%$  carbohydrates,  $22.3 \pm 1.6\%$  proteins,  $17.6 \pm 1.5\%$   
132 lipids, and  $4.0 \pm 0.4\%$  ash (on dry basis). Moreover, the blended FW had a pH of  $6.2 \pm$   
133  $0.1$ , a chemical oxygen demand (COD) content of  $286 \pm 21.9$  g O<sub>2</sub>/kg, and a total (TS)  
134 and volatile (VS) solids content of  $215.6 \pm 1.7$  g/kg and  $207.0 \pm 1.6$  g/kg, respectively.  
135 Finally, the elemental analysis of the FW blend showed the following composition:  $51.2$   
136  $\pm 0.2\%$  carbon,  $8.1 \pm 0.1\%$  hydrogen,  $35.6 \pm 0.9\%$  oxygen,  $3.4 \pm 0.1\%$  nitrogen,  $2.0 \pm$   
137  $0.0\%$  phosphorus and a negligible content of sulphur.

138

## 139 **2.2 Experimental set-up**

140 Continuous hydrogen production via LD-DF was performed in a 1.2-L continuously  
141 stirred tank reactor (CSTR) with 0.8 L of working volume. The body of the reactor was  
142 made of glass PVC, while polypropylene was used for the base and cover. The CSTR  
143 was equipped with sampling ports for both the liquid and gaseous phase (see  
144 Supplementary Material). The amount of acidogenic off-gas evolved was measured by  
145 using an in-house wet gas flow meter based on the water displacement method, which  
146 was interconnected to the reactor using low gas permeability Marprene® and  
147 polyethylene Tubepack® tubing. The CSTR was placed in a temperature-controlled  
148 room at  $37 \pm 1$  °C and magnetically stirred at  $\approx 200$  rpm. A pH controller (BSV,  
149 EVOPH-P-5 model, Spain) was used to measure and maintain constant the operational  
150 pH at  $6.5 \pm 0.1$  by pumping a 6 M NaOH solution on demand (Regueira-Marcos et al.,  
151 2023). Finally, continuous FW feeding and anaerobic broth withdrawal was carried out  
152 by using a time controlled peristaltic pump and a liquid level controlled peristaltic  
153 pump, respectively.

154

## 155 **2.3 Impact of HRT on the performance of continuous lactate-driven dark** 156 **fermentation of food waste**

157 The CSTR was operated for 51 days to assess the influence of HRT and transient  
158 feast/famine perturbations on the FW LD-DF process performance. The response of the  
159 process to changes in the HRT was evaluated during the first 35.4 days of operation,  
160 which were divided into 3 operational stages, i.e., I–III (Table 1). The HRT was  
161 stepwise reduced from 24 to 16 and 12 h, leading to corresponding OLRs values of  
162 99.5, 149.3 and 199 g COD/L-d for stage I, II and III, respectively. The CSTR reactor  
163 was initially operated in batch mode. To that aim, the reactor was filled with 720 mL of  
164 FW and 80 mL of inoculum with a volatile suspended solids (VSS) concentration of



165 0.41 ± 0.05 g/L. The initial TS content of the FW was 7.5% (w/w), as it was previously  
166 found to be optimal for FW LD-DF (Regueira-Marcos et al., 2023). The feeding regime  
167 of the reactor was switched to continuous mode during the exponential phase in regard  
168 to hydrogen production. The CSTR was thus continuously fed at a variable flow rate  
169 depending on the HRT tested. It is noteworthy that the FW supplied was refrigerated at  
170 4 °C and had a constant TS concentration of 7.5% (w/w) throughout the operation.

171 Liquid samples were taken and analysed periodically during operation for the  
172 determination of pH and the concentration of carbohydrates, VS, COD, and organic  
173 acids. Likewise, the flow rate of the gas produced and its composition was periodically  
174 monitored. The volume of hydrogen was adjusted to standard temperature and pressure  
175 conditions (0 °C and 1 atm). The HPR, HY, acidogenic off-gas quality (hydrogen  
176 content), hydrogen production stability index (HPSI), and carboxylic acid profile were  
177 selected as the main process performance indicators. HPSI was calculated as reported  
178 previously by García-Depraect et al. (2020b). The process was also characterized based  
179 on VS, COD and total carbohydrates removal efficiencies, and the requirement of alkali  
180 (expressed in mL OH<sup>-</sup>/g-VS<sub>added</sub> and mL OH<sup>-</sup>/L-d). Energy production rate (kJ/L-d) and  
181 energy production yield (kJ/g-VS<sub>added</sub>) were calculated as reported elsewhere (Martínez-  
182 Mendoza et al., 2023). Pseudo-steady state was considered to occur when HPR  
183 deviation remained within 20% of the mean value for at least three consecutive days.

184 See Supplementary material for a more detailed information about the equations used to  
185 evaluate operational parameters and process performance.

186

#### 187 **2.4 Transient feast/famine perturbations on the performance of continuous lactate-** 188 **driven dark fermentation of food waste**

189 Three consecutive transient feast/famine perturbations (i.e., FF1, FF2, FF3) were  
190 applied during stage IV, from the 35<sup>th</sup> day of operation onwards, to evaluate the  
191 robustness and resilience of the FW LD-DF process. All feast/famine perturbations  
192 consisted of 12 h (equivalent to 1 HRT) of famine followed by continuous feeding at 12  
193 h of HRT (FW feast). Before any process perturbation, the CSTR always showed HPS  
194 indices ≥ 80% for at least 3 consecutive days. The response of the process to transient  
195 fest/famine perturbations was evaluated based on the HPR, HY, hydrogen content in the  
196 gaseous phase, and the organic acids profile. More specifically, the response to famine  
197 perturbations was assessed in four different states, as follows: i) pre-perturbation  
198 pseudo-steady state, which included process data collected prior to the perturbation; ii)  
199 transient perturbation state, which included those process data collected during famine  
200 conditions; iii) recovery state, which included process data collected following feeding  
201 restauration until the start of a new pseudo-steady state, and iv) post-perturbation  
202 pseudo-steady state, which included process data from the new steady state.  
203 Additionally, the process was also characterized based on the settling time, which was  
204 defined as the time required by the process to reach a new pseudo-steady state (HPR  
205 values within 20% tolerance deviation for at least 3 consecutive days) following  
206 perturbation. It is noteworthy to mention that resilience was herein defined as the ability  
207 of the process to return to its steady state following the temporary feast/famine  
208 disturbance, while robustness is referred to the ability of the process to remain stable

209 and at high performance even under adverse perturbations (Stricker and Lanza, 2014).  
210 The higher the robustness of the DF system was, the lower the modification of process  
211 performance indicators by operational perturbations.

212

## 213 **2.4 Analytical methods**

214 The concentrations of TS, VS and total and soluble COD were measured following  
215 standard methods (Eaton, 2005). The characterization of the substrate, in term of  
216 CHN(O)SP, carbohydrate, protein and lipid contents, was performed according to the  
217 methods previously described by Regueira-Marcos et al. (2023). The content of  
218 hydrogen in the acidogenic off-gas was analysed by gas chromatography, employing a  
219 Varian CP-3800 gas chromatograph (GC) equipped with a thermal conductivity detector  
220 (TCD) and a Varian CP-Molsieve 5A capillary column (15 m × 0.53 mm × 15 µm)  
221 interconnected with a Varian CP-PoreBOND Q capillary column (25 m × 0.53 mm × 10  
222 µm) (Alcántara et al., 2015). Helium, at a flow rate of 13 mL/min, was used as the  
223 carrier gas. The GC-TCD was also capable of measuring methane, carbon dioxide and  
224 hydrogen sulphide. Finally, organic acids were analysed by high-performance liquid  
225 chromatography (HPLC) using an Alliance HPLC system (model e2695, USA), which  
226 was equipped with an ultraviolet detector (214 nm) and an Aminex chromatographic  
227 column (HPX-87H, Bio Rad, USA) maintained at 75 °C. A Micro-Guard Cation H +  
228 refill cartridge of 30 × 4.6 mm (Bio Rad, USA) was used as a pre-column. Sulfuric acid  
229 (25 mM), at a flow rate of 0.7 mL/min, was employed as the eluent. The target organic  
230 acids included lactate, acetate, formate, propionate, butyrate, iso-butyrate, valerate, and  
231 iso-valerate.

232

## 233 **2.4 Statistical analysis**

234 One-way ANOVA followed by the Tukey or Kruskal-Wallis test (p-value < 0.05),  
235 depending on the case, was employed to compare the different process performance  
236 measures computed during the operation. Data normality distribution was assessed with  
237 the Shapiro-Wilk test (p-value ≤ 0.05). All the statistical analyses were carried out using  
238 the Statgraphics Centurion software (version 19.2.01).

239

## 240 **3. Results and discussion**

### 241 **3.1 Influence of HRT on the continuous lactate-driven dark fermentation of food** 242 **waste**

#### 243 **3.1.1 Hydrogen production**

244 The key operational parameter tested *viz* HRT exerted a significant effect on process  
245 performance. The HPR achieved during pseudo-steady state at an HRT of 24, 16 and 12  
246 h accounted for  $3.5 \pm 1.0$ ,  $4.2 \pm 0.6$  and  $2.9 \pm 0.6$  L H<sub>2</sub>/L-d, respectively (Table 2). As  
247 shown in Figure 1, the recorded HPR peaked at the beginning of the operation at 9.1 L

248 H<sub>2</sub>/L-d before suddenly decreasing down to 0.7 L H<sub>2</sub>/L-d. This behaviour in HPR is  
249 typically observed in healthy DF systems and tends to occur because hydrogen  
250 production kinetics are promoted batchwise (Regueira-Marcos et al., 2023).  
251 Interestingly, an HRT of 24 h (stage I) led to a much less stable process with fluctuating  
252 HPR values in the range of 1.9 and 4.7 L H<sub>2</sub>/L-d and with a HPSI of 0.71. In stage II, a  
253 clear trend to increase HRP until day 17<sup>th</sup> was observed, wherein reactor feeding was  
254 unfortunately interrupted overnight due to tubing clogging. Following this unforeseen  
255 perturbation, the LD-DF reactor was able to recover, reaching a relatively high HPSI of  
256 0.86. An in-depth analysis of transient feast/famine perturbations is presented in section  
257 3.2. In stage III, the HPR showed a gradual decreasing trend when reducing the HRT  
258 from 16 to 12 h, reaching a new equilibrium state with less than 20% variation in HPR.  
259 This sharply decrease in HPR may be attributed to a transient organic overloading due  
260 to the high OLR (199 g COD/L-d) imposed in stage III, as previously observed Paudel  
261 et al. (2017). The DF process capacity found in this study was very similar to that  
262 reported by Martinez-Mendoza et al. (2023), who assessed the continuous DF of fruit-  
263 vegetable waste at HRTs ranging from 24 down to 6 h using the same biocatalyst. These  
264 authors reported the highest HPR (11.8 NL H<sub>2</sub>/L-d) and HY (95.6 mL H<sub>2</sub>/g-VS<sub>added</sub>) at  
265 an HRT of 9 h with a corresponding OLR value of 136.5 g COD L-d, which is very  
266 similar to the OLR (149.3 g COD/L-d) associated with the best HRT in this study.  
267 Martinez-Mendoza et al. (2023) also observed a marked decrease in HPR at 6 h HRT  
268 and 182 g COD/L-d OLR, the latter parameter being quite similar to the OLR imposed  
269 herein at 12 h HRT (199 g COD/L-d).

270 A statistically significant negative correlation was found between HY and HRT  
271 (Table 2). More specifically, the corresponding HY data recorded in stage I, II and III  
272 were  $48.5 \pm 13.9$ ,  $38.8 \pm 5.35$  and  $20.4 \pm 4.1$  mL H<sub>2</sub>/g-VS<sub>added</sub>, respectively. In terms of  
273 energy recovery, the energy production rate ranged between 37.4 and 53.4 kJ/L-d, while  
274 the computed energy yield was 0.62, 0.49 and 0.26 kJ/g-VS<sub>added</sub> in stage I, II and III,  
275 respectively. Regarding the quality of the off-gas produced, the hydrogen content was  
276 found to be similar in operational stages I and III (57% on average), which was  
277 significantly higher than that computed in stage II ( $53.0 \pm 1.2\%$ ). No methane  
278 production was observed during the entire experiment, which suggested that the short  
279 HRT and pH values imposed washed out methanogenic communities. On the other  
280 hand, the removal efficiencies of VS remained on average at  $50.9 \pm 3.6\%$  throughout  
281 the entire operation. Likewise, the pseudo-steady state carbohydrate and COD removal  
282 efficiencies averaged  $90.7 \pm 2.7$  and  $30.0 \pm 7.0\%$ ,  $86.2 \pm 3.2$  and  $23.8 \pm 1.1\%$ , and  $87.1$   
283  $\pm 1.0$  and  $28.0 \pm 1.2\%$  in stage I, II and III, respectively. These results indicated that the  
284 performance of the LD-DF process was not sufficiently described by the hydrogen  
285 content in the off gas and the removal of VS, COD and carbohydrates provided valuable  
286 information, which is in accordance with previous observations (Martínez-Mendoza et  
287 al., 2022; García-Depraect et al., 2023a). Finally, it was found that the shorter the HRT,  
288 the higher the amount of alkali required for the system to keep pH constant, which  
289 ranged from  $317.7 \pm 56.6$  to  $767.2 \pm 98.0$  mL OH<sup>-</sup>/L-d (Table 2). Interestingly, the  
290 alkali requirements normalised to the amount of VS fed ranged between 4.40 and 5.33  
291 mL OH<sup>-</sup>/g-VS<sub>added</sub> (on average) during operational stages I–III.

292 There are not many reports in the literature dealing with the effect of HRT on the  
293 continuous DF process using FW as substrate. Besides, the conditions and



294 methodologies applied markedly differ from each other, making the benchmarking of  
295 disclosed data difficult. Hydrogen productivity during the DF of FW has been  
296 commonly reported to be in the range of 0.2–1.4 L H<sub>2</sub>/L-d (Villanueva-Galindo et al.,  
297 2023), although there are few recent studies reporting higher HPR (as high as 13 L  
298 H<sub>2</sub>/L-d) (Algapani et al., 2019; Lee et al., 2014; Jung et al., 2022; Regueira-Marcos et  
299 al., 2023). Thus, the LD-DF process can be considered as a promising platform to  
300 produce hydrogen from FW based on the best HPR of 4.2 ± 0.6 L H<sub>2</sub>/L-d achieved in  
301 this study. However, further process optimization with enhanced hydrogen  
302 productivities is still required.

303

### 304 3.1.2 Metabolic profile

305 The profile of carboxylic acids experienced well-defined trends throughout the entire  
306 experiment (Figure 2). Particularly, butyrate and acetate remained at relatively high  
307 concentrations (5.43 ± 0.96 g/L and 5.40 ± 2.17 g/L, respectively) during operational  
308 stages I–III. However, low concentrations of butyrate were detected when HPR slow  
309 down by the day 17<sup>th</sup> and during the putative transient overloading in the beginning of  
310 stage III. According to the PCA analysis, butyrate concentration was found to be  
311 positively correlated with both the HPR and HY, which were clustered together, but it  
312 had a negative association with lactate and acetate (Figure 3). Notably, the  
313 concentration of lactate in the broth skyrocketed from a few milligrams to about 9.8 g/L  
314 while HPR and butyrate plummeted from 6.1 to 1.1 L H<sub>2</sub>/L-d and from 9.1 to 4.3 g/L  
315 during the operational failure that occurred on day 17. This lactate-butyrate-HPR  
316 correlation was confirmed at the beginning of stage III. Therefore, higher HPR values  
317 were closely associated with low titers of lactate and acetate (specially of the former)  
318 and high concentrations of butyrate in the fermentation broth, which reinforced the  
319 hypothesis of hydrogen production via LD-DF (García-Depraect et al., 2021). It has  
320 been reported that during LD-DF, lactate serves as the electron donor while acetate acts  
321 as an oxidant agent (Tao et al., 2016), explaining their close association. The putative  
322 LD-DF mechanism starts with the oxidation of lactate to acetate and carbon dioxide (or  
323 a derivative thereof), and the subsequent formation of butyrate by condensation of two  
324 moles of acetate to produce an intermediate compound that is ultimately reduced to  
325 butyrate (García-Depraect et al., 2021). The behaviour of propionate, which was  
326 detected throughout the operation at average broth concentrations of 2.24 ± 0.99 g/L,  
327 was also unexpected. It is commonly recognized that propionate acts as a hydrogen sink  
328 during DF, which can be produced either from the fermentation of carbohydrates or  
329 lactate (Grause et al., 2012; Fuess et al., 2018). Here it seems that propionate was  
330 negatively related to lactate (Figure 3). It has been reported that propionate can be  
331 produced from lactate, thereby leading to lower hydrogen production (Chen et al., 2019;  
332 Sim et al., 2022). Sim et al. (2019) avoided the conversion of lactate to propionate by  
333 *Megasphaera elsdenii* by bioaugmenting the process with *Clostridium butyricum* which  
334 can oxidase lactate to hydrogen. Other soluble metabolite identified over the course of  
335 the process was iso-valerate, with concentrations ranging from 2.1 g/L in stage I to 0.15  
336 g/L in stage III, regardless of the behaviour of hydrogen production, suggesting that the  
337 production of iso-valerate did not significantly affect the electron flux toward hydrogen.

338

## 339 **3.2 Influence of feast-famine perturbations on the continuous lactate-driven dark** 340 **fermentation of food waste**

### 341 **3.2.1 Hydrogen production during transient feast/famine perturbations**

342 Feast/famine perturbations did not cause a severe deterioration on the degradation  
343 efficiency of carbohydrates and VS, which varied between 71.3 and 93.4 % and  
344 between 43.2 and 52.0 %, respectively. Hydrogen content in the acidogenic off-gas was  
345 slightly reduced only during famine conditions, from  $52.3 \pm 2.5\%$  down to  $41.5 \pm 1.7\%$ ,  
346 but it rapidly returned to previous values after FW feeding resumption. However, all the  
347 three feast/famine perturbations intentionally applied led to a similar process's  
348 behaviour, which was characterized by a significant reduction in HPR during famine  
349 operation followed by an up-down HPR response following perturbation and  
350 subsequent HPR stabilization (Figure 4). It is also worth noting that the HY response to  
351 feast/famine perturbations showed a similar trend to the one observed for HPR, pointing  
352 out that the LD-DF process had the ability to bounce back from perturbation (Figure 4).  
353 Previous studies have also pointed out the resilience of dark fermenters against different  
354 types of stresses such a sudden pH acidification/alkalinization, organic overloading,  
355 substrate composition, and starvation (Park et al. 2015; Monroy et al., 2018; García-  
356 Depraect et al., 2020a).

357 Four different stages were defined using HPR as target process indicator, i.e., i)  
358 initial pseudo-steady state, ii) transient perturbation state, iii) recovery state, and iv)  
359 post-perturbation pseudo-steady state in order to have a deeper in-sight in the  
360 feast/famine perturbation effect. The preceding steady state HPR value of 2.9, 2.8, and  
361 3.7 L H<sub>2</sub>/L-d was used as reference for FF1, FF2 and FF3, respectively. A ratio between  
362 the HPR recorded during the four different stages and the reference HPR higher than 1  
363 indicates a global process enhancement, while a global HPR reduction can be inferred  
364 from a ratio lower than 1 (Table 3). On average, the HPR recorded under starvation  
365 conditions (transient perturbation state) decreased to  $0.7 \pm 0.3$  L H<sub>2</sub>/L-d. Interestingly,  
366 when comparing the HPR achieved during transient perturbation state with the steady-  
367 state HPR computed prior to perturbation, a more pronounced decrease in HPR was  
368 observed as perturbations were applied, pointing out that the process became more  
369 susceptible to starvation as feast/famine operation progressed. During the recovery state  
370 (which lasted for 2.13, 1.31 and 1.35 for FF1, FF2, and FF3, respectively) HPR  
371 suddenly peaked to 10.1, 19.2 and 7.7 L H<sub>2</sub>/L-d and rapidly levelled off reaching a new  
372 steady state. The underlying mechanisms of the observed behaviour need to be further  
373 investigated. However, the r/K selection theory could explain in some extent the sudden  
374 increase in HPR recorded. In this regard, lactate-oxidizing-HPB are classified as r-  
375 strategists with high growth rate and a competitive advantage in resource-rich  
376 environments. In contrast, LAB are suggested to be K-strategists with a high biomass  
377 specific uptake rate for fermentable carbohydrates (Kim et al., 2021). Thus, it was  
378 hypothesized that temporary starvation and subsequent feeding somewhat improved the  
379 activity of lactate-oxidizing -HPB, which could explain the HPR patterns observed  
380 during the transient perturbation state and the recovery state. The assumption of an  
381 enhanced hydrogen-producing activity could also endorse the behaviour of HPR  
382 identified during the post-perturbation pseudo-steady state. The HPR computed after  
383 perturbation was similar to the reference HPR value in FF1, and 33 and 17% higher in  
384 FF2 and FF3, respectively. This entailed an increase in hydrogen productivity after

385 three feast/famine stresses despite an HRT of 12 h was not the best operating condition,  
386 as discussed previously in section 3.1.

387

### 388 **3.2.2 Metabolic profile during transient feast/famine perturbations**

389 The transient feast/famine perturbations impacted not only the hydrogen production  
390 performance but also the profile of organic acids (Figure 3). Compared to an HRT of 16  
391 h, an HRT of 12 h was found to be more conducive to the accumulation of lactate and  
392 acetate, but not of butyrate and propionate. Interestingly, all perturbation events applied  
393 resulted in a sudden and drastic decrease in lactate and acetate levels, and increases in  
394 butyrate, propionate and, to a lesser extent formate, after feeding restoration, which  
395 agrees with previous observations (Monroy et al., 2018). Hence, feast/famine  
396 perturbations likely triggered bacterial acidogenic activity, leading to a peak in the  
397 alkali requirement (Figure 4). In the LD-DF process, hydrogen production is closely  
398 related to the evolution of lactate. The low levels of lactate (electron donor) and acetate  
399 (acceptor donor) observed during the recovery state seems to reinforce the assumption  
400 that transient feast/famine cycles fostered, at least temporarily, the activity of lactate-  
401 oxidizing-HPB (Tao et al., 2016; Fuess et al., 2018). As discussed previously, the  
402 operational failure on day 17 is very illustrative for that case (Figure 2). In LD-DF, it  
403 has been argued that low concentrations of lactate in the broth are an indicator of an  
404 efficient process (García-Depraect et al., 2021). Thus, the fact that the broth  
405 concentrations of lactate and acetate slowly returned to high concentrations during the  
406 post-perturbation pseudo-steady state was likely attributed to the suboptimal HRT/OLR  
407 condition imposed (Paudel et al., 2017). Therefore, it can be hypothesized that 12 h of  
408 HRT boosted the activity of LAB over HPB, which would lead to a gradual  
409 accumulation of lactate under long term operation.

410 **In brief**, the present LD-DF study targeted an enhanced hydrogen production  
411 from FW. This alternative hydrogen-producing approach can cope with the inhibition  
412 issues related to the overgrowth of LAB, which typically outcompete HPB for  
413 fermentable carbohydrates (García-Depraect et al., 2021; Canto-Robertos et al., 2023).  
414 This study also helped filling the knowledge gap of continuous LD-DF of organic  
415 waste, which has been commonly studied in batch mode (e.g., Martínez-Mendoza et al.,  
416 2022; Lois-Regueira et al., 2023). The LD-DF process herein evaluated resulted in  
417 relatively high hydrogen productivities and confirmed the key role of HRT on stable  
418 process performance. Additionally, the LD-DF process was tested against temporary  
419 feast/famine disturbances, mimicking a stress that could occur in large DF plants.  
420 Despite the process rapidly deteriorated during famine periods, leading to low hydrogen  
421 production, the LD-DF exhibited a high resilience. Although the Readiness Technology  
422 Level (RTL) of DF is 5-6, it is expected that some unforeseen and/or foreseen  
423 perturbations can exist in further large-scale systems. In this line, further studies should  
424 focus on the impact of different operational perturbations, e.g., shocks in pH, organic  
425 load, temperature, and long starvation, etc, on process performance and the structure of  
426 the microbial populations. One of the weaknesses of this study was the use of synthetic  
427 organic recipe, which was used in the proof of concept of the continuous hydrogen  
428 production from FW via LD-DF. It is thus highly recommended to conduct further  
429 validation studies using real FW, which is expected to be more complex than the recipe-

430 based FW. Real FW would present a high autochthonous bacteria load, be highly  
431 heterogenous and pre-acidified at some extent, all of which can impact the process.  
432 Finally, it must be pointed out that the peak in HPR observed during the transient state  
433 following famine conditions along with the associated profile of lactate strongly  
434 suggested that an adequate balance between LAB and lactate-oxidizing-HPB is crucial  
435 to support a high hydrogen production rate. Further studies should not only perform  
436 molecular analyses to get an in-depth knowledge of the microbiome involved but also to  
437 bridge the gap between process design and strategy and microbial and ecological  
438 aspects. The development of novel strategies aiming at improving the syntrophic  
439 association between LAB and HPB can further boost the high HPR herein achieved.

440

#### 441 **4. Conclusions**

442 The influence of the HRT on the continuous LD-DF of FW was investigated for the first  
443 time. The best hydrogen production performance was found at 16 h of HRT, leading to  
444 a more stable operation and a HPR of 4.2 L H<sub>2</sub>/L-d. Lactate consumption was identified  
445 as the main hydrogen-producing pathway rather than the one-step fermentation of  
446 carbohydrates. Further operation under temporary feast/famine perturbations evidenced  
447 a poor robustness of the process, but it exhibited a prominent resilient capacity  
448 following the disturbed operation. Overall, the LD-DF process supported promising  
449 results for the further optimization of continuous hydrogen production from real FW.

450

451 E-supplementary data for this work can be found in the e-version of this paper online.

452

#### 453 **Acknowledgments**

454 This work has received funding from the European Union's Horizon 2020 research and  
455 innovation programme under the Marie Skłodowska-Curie grant agreement No. 894515.  
456 The work was also supported by Grant RYC2021-034559-I funded by MCIN/AEI  
457 /10.13039/501100011033 and by European Union NextGenerationEU/PRTR. The  
458 regional government of Castilla y León and the European FEDER Programme (CLU  
459 2017-09, CL-EI-2021-07 and UIC 315) are also acknowledged for their support. The  
460 co-financial support of the "Consejería de Educación" of the regional government of  
461 Castilla y León and the European Social Fund are also acknowledged.

462

#### 463 **5. References**

- 464 [1] Alcántara, C., Fernández, C., García-Encina, P.A., Muñoz, R., 2015. Mixotrophic  
465 metabolism of *Chlorella sorokiniana* and algal-bacterial consortia under extended dark-  
466 light periods and nutrient starvation. *Appl. Microbiol. Biotechnol.* 99, 2393–2404.  
467 [2] Algapani, D.E., Qiao, W., Ricci, M., Bianchi, D., Wandera, S.M., Adani, F.,  
468 Dong, R., 2019. Bio-hydrogen and bio-methane production from food waste in a two-

- 469 stage anaerobic digestion process with digestate recirculation. *Renew. Energ.* 130,  
470 1108–1115.
- 471 [3] Battista, F., Frison, N., Pavan, P., Cavinato, C., Gottardo, M., Fatone, F., Eusebi,  
472 A.L. Majone, M., Zeppilli, M., Valentino, F., Fino, D., Tommasi, T., Bolzonella, D.,  
473 2020. Food wastes and sewage sludge as feedstock for an urban biorefinery producing  
474 biofuels and added-value bioproducts. *J. Chem. Technol. Biotechnol.* 95(2), 328–338.
- 475 [4] Canto-Robertos, M., Quintal-Franco, C., Ponce-Caballero, C., Vega-De Lille, M.,  
476 Moreno-Andrade, I., 2023. Inhibition of hydrogen production by endogenous  
477 microorganisms from food waste. *Braz. J. Chem. Eng.* 40(1), 137–150.
- 478 [5] Chen, L., Shen, Y., Wang, C., Ding, L., Zhao, F., Wang, M., Fu, J., Wang, H.,  
479 2019. *Megasphaera elsdenii* lactate degradation pattern shifts in rumen acidosis models.  
480 *Front. Microbiol.* 10, 162.
- 481 [6] Cheng, D., Ngo, H.H., Guo, W., Chang, S.W., Nguyen, D.D., Deng, L., Chen, Z.,  
482 Ye, Y., Bui, X.T., Hoang, N.B., 2022. Advanced strategies for enhancing dark  
483 fermentative biohydrogen production from biowaste towards sustainable environment.  
484 *Bioresour. Technol.* 351, 127045.
- 485 [7] Dawood, F., Anda, M., Shafiullah, G.M., 2020. Hydrogen production for energy:  
486 An overview. *Int. J. Hydrog. Energy* 45, 3847–3869.
- 487 [8] Detman, A., Mielecki, D., Chojnacka, A., Salamon, A., Błaszczuk, M.K., Sikora,  
488 A., 2019. Cell factories converting lactate and acetate to butyrate: *Clostridium*  
489 *butyricum* and microbial communities from dark fermentation bioreactors. *Microb. Cell*  
490 *Factories* 18, 36.
- 491 [9] Eaton, A.D., Clesceri, L.S., Greenberg, A.E., 2005. Standard methods for the  
492 examination of water and wastewater, 21<sup>st</sup> ed. American Public Health  
493 Association/American Water Works Association/Water Environment Federation,  
494 Washington DC.
- 495 [10] European Commission, Directorate-General for Energy, 2020. Communication  
496 from the commission to the European parliament, the council, the European economic  
497 and social committee and the committee of the regions a hydrogen strategy for a  
498 climate-neutral Europe. [https://eur-lex.europa.eu/legal-](https://eur-lex.europa.eu/legal-content/EN/ALL/?uri=CELEX:52020DC0301)  
499 [content/EN/ALL/?uri=CELEX:52020DC0301](https://eur-lex.europa.eu/legal-content/EN/ALL/?uri=CELEX:52020DC0301).
- 500 [11] Eurostat. 2022. Food waste: 127 kg per inhabitant in the EU in 2020.  
501 <https://ec.europa.eu/12urostat/web/products-eurostat-news/-/ddn-20220925-2>.
- 502 [12] Fattibene, D., Recanati, F., Dembska, K., Antonelli, M., 2020. Urban food waste:  
503 A framework to analyse policies and initiatives. *Resources* 9(9), 99.
- 504 [13] Fuess, L.T., Júnior, A.D.N.F., Machado, C.B., Zaiat, M., 2018. Temporal  
505 dynamics and metabolic correlation between lactate-producing and hydrogen-producing  
506 bacteria in sugarcane vinasse dark fermentation: the key role of lactate. *Bioresour.*  
507 *Technol.* 247, 426–433.
- 508 [14] García-Depraect, O., Diaz-Cruces, V. F., Rene, E. R., León-Becerril, E., 2020a.  
509 Changes in performance and bacterial communities in a continuous biohydrogen-  
510 producing reactor subjected to substrate-and pH-induced perturbations. *Bioresour.*  
511 *Technol.* 295, 122182.
- 512 [15] García-Depraect, O., Muñoz, R., van Lier, J. B., Rene, E. R., Diaz-Cruces, V. F.,  
513 León-Becerril, E., 2020b. Three-stage process for tequila vinasse valorization through  
514 sequential lactate, biohydrogen and methane production. *Bioresour. Technol.* 307,  
515 123160.



- 516 [16] García-Depraect, O., Castro-Muñoz, R., Muñoz, R., Rene, E.R., León-Becerril,  
517 E., Valdez-Vazquez, I., Gopalakrishnan, K., Reyes-Alvarado, L.C., Martínez-Mendoza,  
518 L.J., Carillo-Reyes, J., Buitrón, G., 2021. A review on the factors influencing  
519 biohydrogen production from lactate: The key to unlocking enhanced dark fermentative  
520 processes. *Bioresour. Technol.* 324, 124595.
- 521 [17] García-Depraect, O., Mena-Navarro, V., Muñoz, R., Rene, E. R., León-Becerril,  
522 E., 2023a. Effect of nitrogen and iron supplementation on the process performance and  
523 microbial community structure of a hydrogen-producing reactor continuously fed with  
524 tequila vinasse. *Fuel* 334, 126736.
- 525 [18] García-Depraect, O., Mirzazada, I., Martínez-Mendoza, L. J., Regueira-Marcos,  
526 L., Muñoz, R., 2023b. Biotic and abiotic insights into the storage of food waste and its  
527 effect on biohydrogen and methane production potential. *J. Water Process Eng.* 53,  
528 103840.
- 529 [19] Grause, G., Igarashi, M., Kameda, T., Yoshioka, T., 2012. Lactic acid as a  
530 substrate for fermentative hydrogen production. *Int. J. Hydrog. Energy* 37(22), 16967–  
531 16973.
- 532 [20] Habashy, M.M., Ong, E.S., Abdeldayem, O.M., Al-Sakkari, E.G., Rene, E.R.,  
533 2021. Food waste: a promising source of sustainable biohydrogen fuel. *Trends*  
534 *Biotechnol.* 39(12), 1274–1288.
- 535 [21] Jung, J.-H., Sim, Y.-B., Ko, J., Park, S.Y., Kim, G.-B., Kim, S.-H., 2022.  
536 Biohydrogen and biomethane production from food waste using a two-stage dynamic  
537 membrane bioreactor (DMBR) system. *Bioresour. Technol.* 352, 127094.
- 538 [22] Kim, D.-H., Park, J.-H., Kim, S.-H., Kumar, G., Lee, B.-D., Kumar, S., Yoon, J.-  
539 J., 2021. Shift of microbial community structure by substrate level in dynamic  
540 membrane bioreactor for biohydrogen production. *Int. J. Energy Res.* 45(12), 17408–  
541 17416.
- 542 [23] Lee, C., Lee, S., Han, S.-K., Hwang, S., 2014. Effect of operational pH on  
543 biohydrogen production from food waste using anaerobic batch reactors. *Water Sci.*  
544 *Technol.* 69, 1886–1893.
- 545 [24] Martínez-Mendoza, L.J., Lebrero, R., Muñoz, R., García-Depraect, O., 2022.  
546 Influence of key operational parameters on biohydrogen production from fruit and  
547 vegetable waste via lactate-driven dark fermentation. *Bioresour. Technol.* 364, 128070.
- 548 [25] Martínez-Mendoza, L.J., García-Depraect, O., Muñoz, R., 2023. Unlocking the  
549 high-rate continuous performance of fermentative hydrogen bioproduction from fruit  
550 and vegetable residues by modulating hydraulic retention time. *Bioresour. Technol.*  
551 373, 128716.
- 552 [26] Monroy, I., Bakonyi, P., Buitrón, G., 2018. Temporary feeding shocks increase  
553 the productivity in a continuous biohydrogen-producing reactor. *Clean Technol.*  
554 *Environ. Policy.* 20, 1581–1588.
- 555 [27] Neves, L., Gonçalo, E., Oliveira, R., Alves, M.M., 2008. Influence of composition  
556 on the biomethanation potential of restaurant waste at mesophilic temperatures. *Waste*  
557 *Manage.* 28, 965–972.
- 558 [28] Ohnishi, A., Hasegawa, Y., Fujimoto, N., Suzuki, M., 2022. Biohydrogen  
559 production by mixed culture of *Megasphaera elsdenii* with lactic acid bacteria as  
560 lactate-driven dark fermentation. *Bioresour. Technol.* 343, 126076.
- 561 [29] Park, J.-H., Kumar, G., Park, J.-H., Park, H.-D., Kim, S.-H., 2015. Changes in  
562 performance and bacterial communities in response to various process disturbances in a  
563 high-rate biohydrogen reactor fed with galactose. *Bioresour. Technol.* 188, 109–116.

- 564 [30] Park, J.-H., Kim, D.-H., Baik, J.-H., Park, J.-H., Yoon, J.-J., Lee, C.-Y., Kim, S.-  
565 H., 2021. Improvement in H<sub>2</sub> production from *Clostridium butyricum* by co-culture with  
566 *Sporolactobacillus vineae*. Fuel 285, 119051.
- 567 [31] Paudel, S., Kang, Y., Yoo, Y.-S., Seo, G.T., 2017. Effect of volumetric organic  
568 loading rate (OLR) on H<sub>2</sub> and CH<sub>4</sub> production by two-stage anaerobic co-digestion of  
569 food waste and brown water. Waste Manage. 61, 484–493.
- 570 [32] Pérez-Rangel, M., Barboza-Corona, J.E., Navarro-Díaz, M., Escalante, A.E.,  
571 Valdez-Vazquez, I., 2021. The duo *Clostridium* and *Lactobacillus* linked to hydrogen  
572 production from a lignocellulosic substrate. Water Sci. Technol. 83(12), 3033–3040.
- 573 [33] Regueira-Marcos, L., García-Depraect, O., Muñoz, R., 2023. Elucidating the role  
574 of pH and total solids content in the co-production of biohydrogen and carboxylic acids  
575 from food waste via lactate-driven dark fermentation. Fuel 338, 127238.
- 576 [34] Scherhauser, S., Moates, G., Hartikainen, H., Waldron, K., Obersteiner G., 2018.  
577 Environmental impacts of food waste in Europe. Waste Manage. 77, 98–113.
- 578 [35] Sikora, A., Błaszczuk, M., Jurkowski, M., Zielenkiewicz, U., 2013. Lactic acid  
579 bacteria in hydrogen-producing consortia: on purpose or by coincidence?, in: Kongo,  
580 J.M. (Ed.), Lactic Acid Bacteria - R & D for Food, Health and Livestock Purposes.  
581 IntechOpen, Croatia, pp. 488–514.
- 582 [36] Shanmugam, S., Mathimani, T., Rajendran, K., Sekar, M., Rene, E.R., Chi,  
583 N.T.L., Ngo, H.G., Pugazhendhi, A., 2023. Perspective on the strategies and challenges  
584 in hydrogen production from food and food processing wastes. Fuel 338, 127376.
- 585 [37] Sim, Y.-B., Yang, J., Joo, H. H., Jung, J.-H., Kim, D.-H., Kim, S.-H., 2022. Effect  
586 of bioaugmentation using *Clostridium butyricum* on the start-up and the performance of  
587 continuous biohydrogen production. Bioresour. Technol. 366, 128181.
- 588 [38] Sivagurunathan, P., Kumar, G., Bakonyi, P., Kim, S.-H., Kobayashi, T., Xu, K.Q.,  
589 Lakner, G., Tóth, G., Nemestóthy, N., Bélafi-Bakó, K., 2016. A critical review on  
590 issues and overcoming strategies for the enhancement of dark fermentative hydrogen  
591 production in continuous systems. Int. J. Hydrog. Energy 41(6), 3820–3836.
- 592 [39] Stricker, N., Lanza, G., 2014. The concept of robustness in production systems  
593 and its correlation to disturbances. Procedia CIRP 19, 87–92.
- 594 [40] Talan, A., Tiwari, B., Yadav, B., Tyagi, R.D., Wong, J.W.C., Drogui, P., 2021.  
595 Food waste valorization: Energy production using novel integrated systems. Bioresour.  
596 Technol. 322, 124538.
- 597 [41] Tao, Y., Hu, X., Zhu, X., Jin, H., Xu, Z., Tang, Q., Li, X., 2016. Production of  
598 butyrate from lactate by a newly isolated *Clostridium* sp. BPY5. Appl. Biochem.  
599 Biotechnol. 179, 361–374.
- 600 [42] Villanueva-Galindo, E., Vital-Jácome, M., Moreno-Andrade, I., 2023. Dark  
601 fermentation for H<sub>2</sub> production from food waste and novel strategies for its  
602 enhancement. Int. J. Hydrog. Energy 48(27), 9957–9970.
- 603 [43] Yun, Y.-M., Lee, M.-K., Im, S.-W., Marone, A., Trably, E., Shin, S.-R., Kim, M.-  
604 G., Cho, S.-K., Kim, D.-H., 2018. Biohydrogen production from food waste: current  
605 status, limitations, and future perspectives. Bioresour. Technol. 248, 79-87.
- 606 [44] Zabaniotou, A., Kamaterou, P., 2019. Food waste valorization advocating Circular  
607 Bioeconomy – A critical review of potentialities and perspectives of spent coffee  
608 grounds biorefinery. J. Clean. Prod. 211, 1553–1566.

609  
610  
611

612  
613  
614  
615  
616  
617  
618

**Figure captions:**

619 **Fig. 1.** Time course of A) hydrogen production rate (HPR), hydrogen content, and  
620 volatile solids (VS) and total carbohydrates (CH) removal, and B) hydrogen yield (HY)  
621 and alkali requirement during the continuous LD-DF of FW. Vertical dotted lines stand  
622 for the shifts in HRT (24, 18 and 12 h for stage I, II and III, respectively).

623 **Fig. 2.** Time course of organic acids concentration and HPR during the continuous LD-  
624 DF of FW at decreasing HRTs (24, 18 and 12 h for stage I, II and III, respectively).

625 **Fig. 3.** Principal component analysis (PCA) based on the evolution in HPR, HY and the  
626 concentration of lactate, acetate, propionate and butyrate at decreasing HRTs (24, 18  
627 and 12 h for stage I, II and III, respectively).

628 **Fig. 4.** Time course of A) hydrogen production rate (HPR), hydrogen content, and  
629 volatile solids (VS) and total carbohydrates (CH) removal, and B) hydrogen yield (HY)  
630 and alkali requirement during the feast/famine perturbations applied in the continuous  
631 LD-DF of FW. Vertical shaded bars indicate the length of famine condition.

632 **Fig. 5.** Time course of organic acids concentration and HPR during the feast/famine  
633 perturbations applied in the continuous LD-DF of FW. Vertical shaded bars indicate the  
634 length of famine condition.

635 **Table 1.** Summary of the operating conditions tested during the continuous LD-DF of  
 636 FW.

Parameter	Stage I	Stage II	Stage III	Stage IV
Time (days)	0–11.4	11.4–26.0	26.0–35.4	35.4–51.0
HRT (h)	24	16	12	12
OLR (g VS/L-d)	72.0	108.0	144.0	144.0
OLR (g COD/L-d)	99.5	149.25	199.0	199.0
HRT cycles (-)	11.4	21.9	18.8	31.2

637 **Note:** Stages I to III aimed at investigating the effect of HRT on the continuous LD-DF  
 638 of FW, while stage IV was devoted to the study process performance under transient  
 639 feast/famine perturbations. HRT: Hydraulic retention time; OLR: Organic loading rate;  
 640 COD: Chemical oxygen demand.

641

642 **Table 2.** Summary of the process performance indicators collected during the  
 643 continuous FW LD-DF process.

Parameter	Stage I	II	III
<b>HRT</b>	24	16	12
<b>HPR (L H<sub>2</sub>/L-d)</b>	3.5 ± 1.0 ab	4.2 ± 0.6 a	2.9 ± 0.6 b
<b>HY (mL H<sub>2</sub>/g-VS<sub>added</sub>)</b>	48.5 ± 13.9a	38.8 ± 5.35b	20.4 ± 4.1c
<b>H<sub>2</sub> content (%)</b>	56.5 ± 2.9a	53.0 ± 1.2b	56.9 ± 2.2a
<b>VS<sub>removal</sub> (%)</b>	52.5 ± 6.3	49.8 ± 2.5	51.8 ± 3.6
<b>CH<sub>removal</sub> (%)</b>	90.7 ± 2.7	86.2 ± 3.2	87.1 ± 1.0
<b>COD<sub>removal</sub> (%)</b>	30.0 ± 7.0	23.8 ± 1.1	28.0 ± 1.2
<b>Alkali requirement (mL OH<sup>-</sup> L/L-d)</b>	317.1 ± 56.6a	507.7 ± 66.8b	762.2 ± 98.1c
<b>Alkali requirement (mL OH<sup>-</sup>/g-VS<sub>added</sub>)</b>	4.4 ± 0.8a	4.7 ± 0.6ab	5.3 ± 0.7b
<b>Energy production rate (kJ/L-d)</b>	44.5 ± 12.7ab	53.4 ± 7.4a	37.4 ± 7.5b
<b>Energy yield (kJ/g-VS<sub>added</sub>)</b>	0.62 ± 0.18a	0.49 ± 0.07b	0.26 ± 0.05c

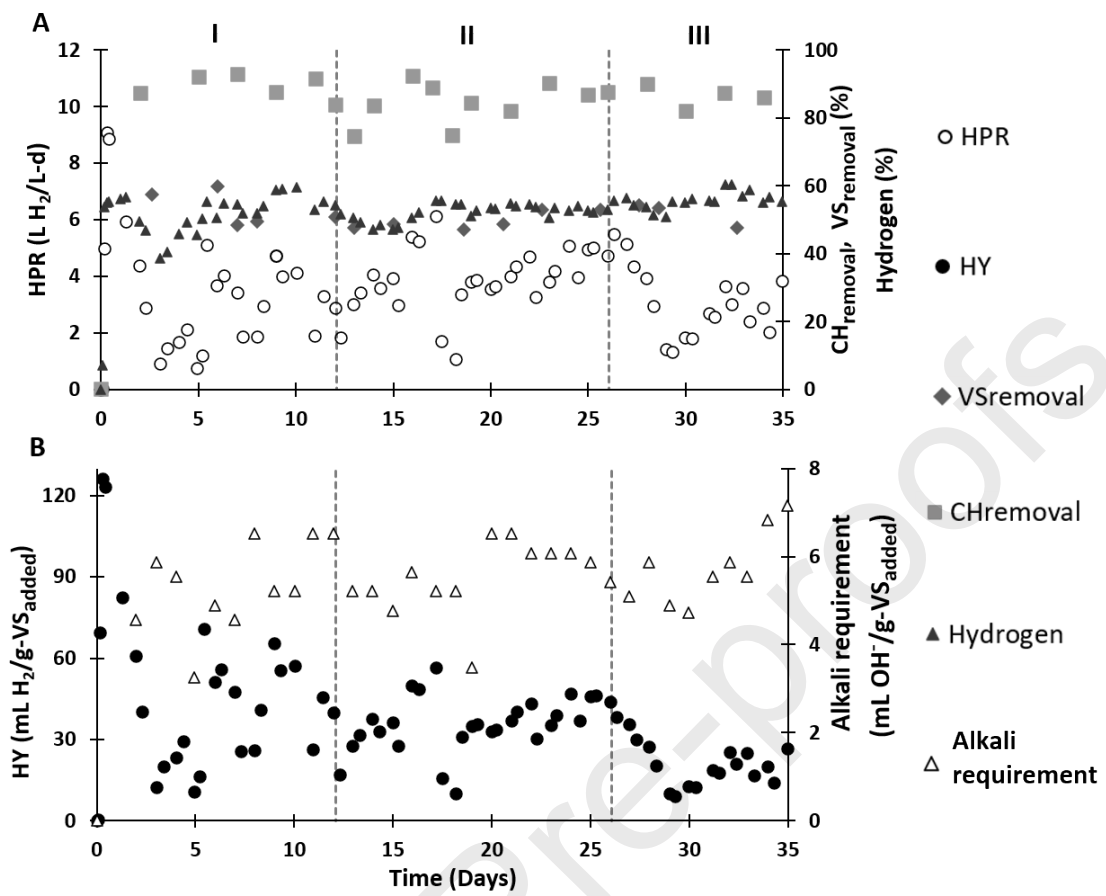
644 **Note:** HRT: Hydraulic retention time; HPR: Hydrogen production rate; HY: hydrogen  
 645 yield. Mean and deviation data is reported during pseudo-steady state, which lasted for  
 646 3.1, 7.0 and 4.3 days in stage I, II and III, respectively. Means with the same letter in the  
 647 same row do not differ significantly ( $p \leq 0.05$ ). The sample size was 6, 15 and 10 for  
 648 stage I, II and III, respectively.



649 **Table 3.** Summary of hydrogen productivities achieved from the LD-DF of FW during  
 650 the different stages assessed under feast/famine perturbations.

Condi tion	Settling period (Days)	TPS (L H <sub>2</sub> /L- d)	TPS/ referenc e	RS (L H <sub>2</sub> /L- d)	RS/ referenc e	PPSS (L H <sub>2</sub> /L- d)	PPSS/ referenc e
FF1	2.13	1.03	0.68	7.2	2.46	2.8	0.96
FF2	1.31	0.65	0.23	10.80	3.90	3.7	1.33
FF3	1.35	0.39	0.11	5.5	1.48	4.3	1.17
Average	1.6 ± 0.5	0.69 ± 0.32	0.3 ± 0.3	7.9 ± 2.7	2.6 ± 1.2	3.6 ± 0.8	1.2 ± 0.2

651 **Note:** *Settling time* is defined as the time required by the process to reach a new pseudo-  
 652 steady state following perturbation. *TPS* (transient perturbation state): HPR recorded  
 653 along the 12-h starvation period. *RS* (recovery state): HPR computed during the settling  
 654 period. *PPSS* (post-perturbation pseudo-steady state): average HPR achieved during a  
 655 new steady state after perturbation. *TPS/reference*, *RS/reference* and *PPSS/reference*  
 656 indicate the ratio between the value of HPR attained in TPS, RS or PPSS and the  
 657 immediately preceding pseudo-steady HPR value. The steady-state HPR data recorded  
 658 prior to FF1, FF2 and FF3 were used as the reference. For interpretation of the obtained  
 659 ratios, the reader is kindly referred to section 3.2.1.

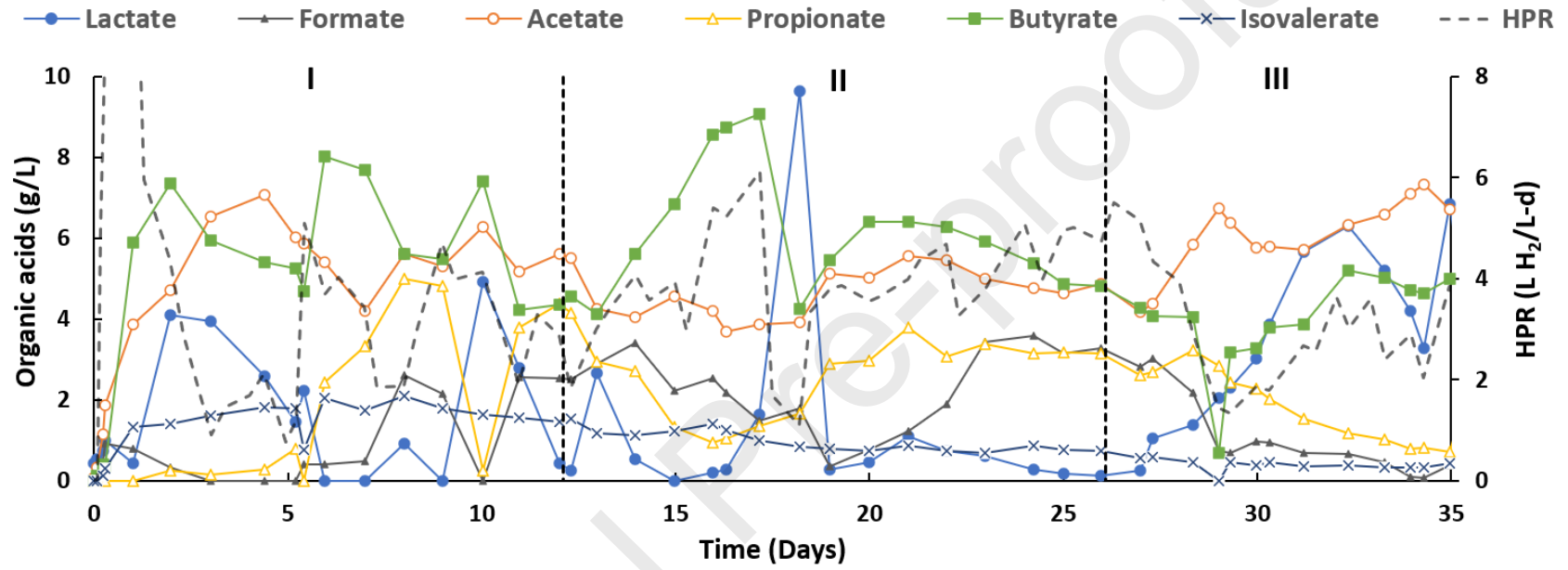


660

661

Figure 1

662

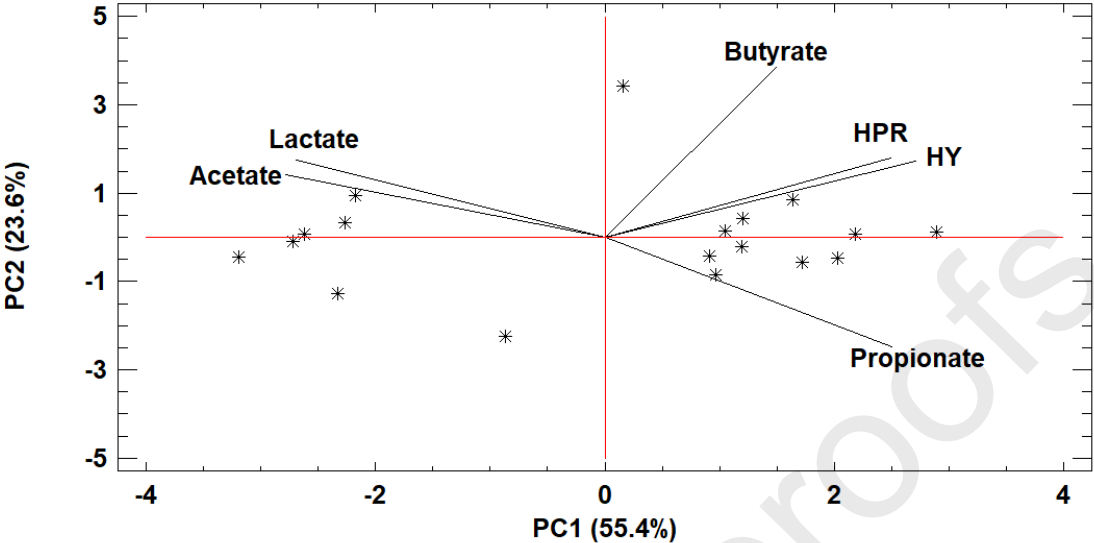


663

664

Figure 2

665

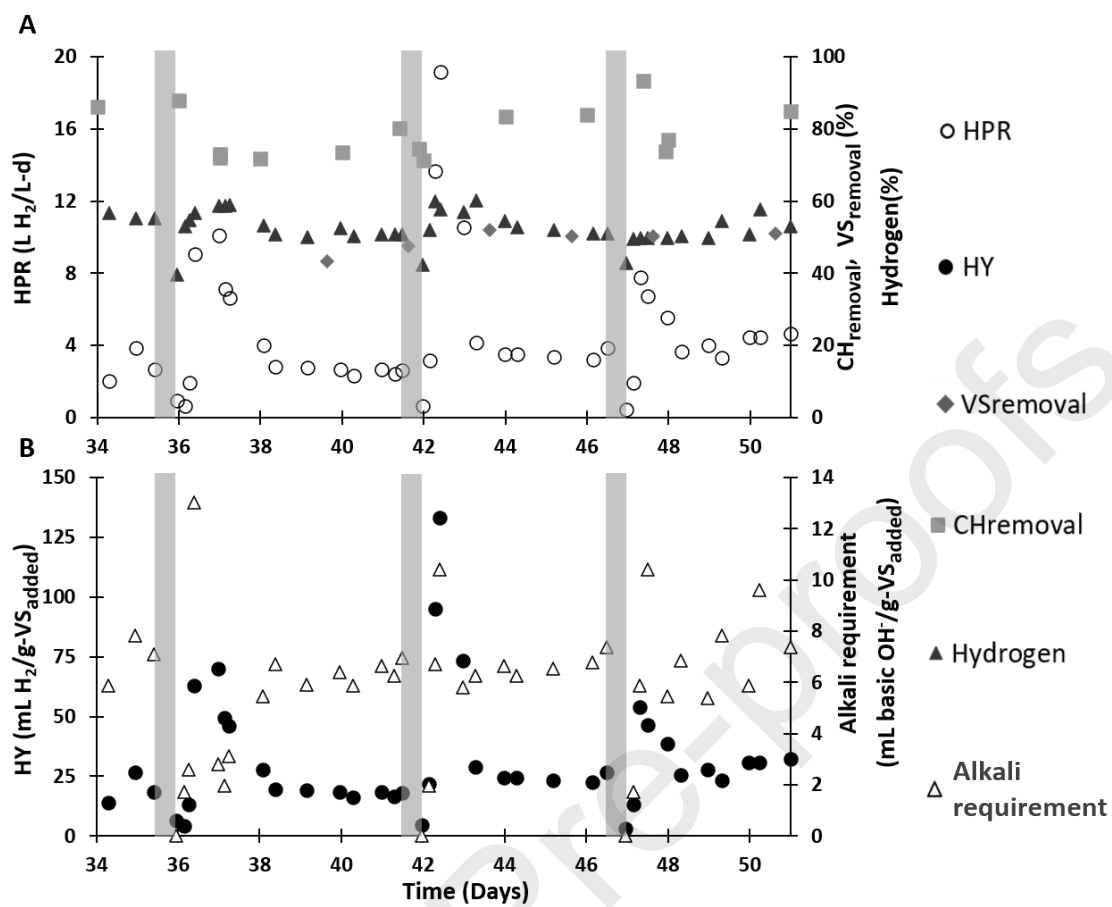


666

667

Figure 3

Journal Pre-proofs



668

669

Figure 4



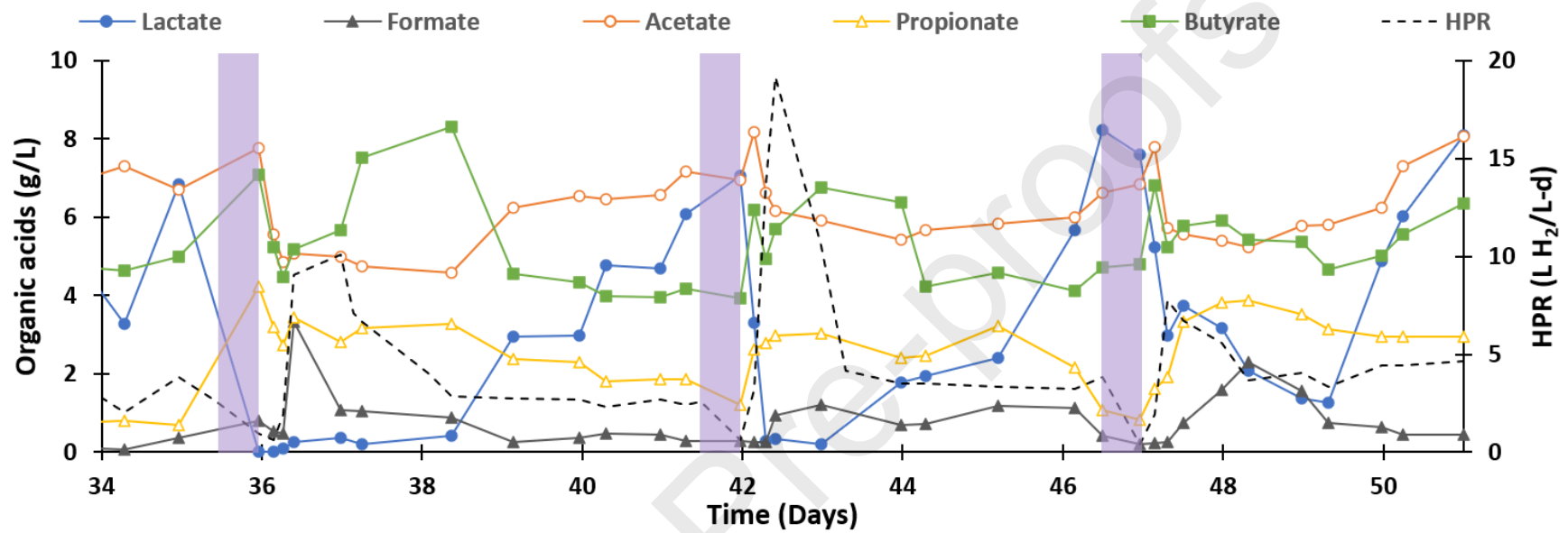


Figure 5

670

671

672 **Declaration of interests**

673

674  The authors declare that they have no known competing financial interests or personal relationships that could have appeared to influence the  
 675 work reported in this paper.

676

677  The authors declare the following financial interests/personal relationships which may be considered as potential competing interests:

678

679

680

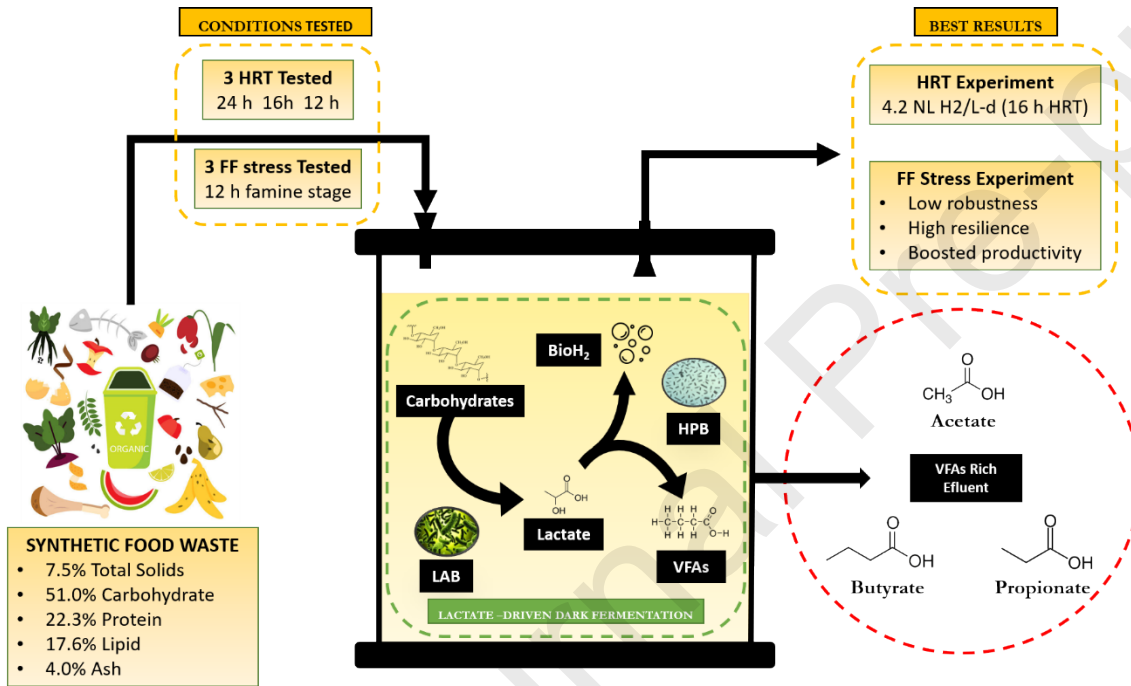
681

682

683

684

685 **Graphical Abstract**



686

687

688 **Highlights**

- 689
- 690
- 691
- 692
- 693
- LD-DF showed high potential for continuous H<sub>2</sub> production from simulated FW
  - HRT impacted on LD-DF, with maximum HPR of 4.2 ± 0.6 NL H<sub>2</sub>/L-d at 16 h
  - Feast/Famine stress resulted in low robustness of HPR against the perturbation
  - Fast stability recovery after perturbation highlighted LD-DF as resilient process
  - High HPRs correlated with lactate/acetate consumption and butyrate production

694

Journal Pre-proofs